

# Targeted Synthesis of a Porous Aromatic Framework with High Stability and Exceptionally High Surface Area\*\*

Teng Ben, Hao Ren, Shengqian Ma, Dapeng Cao, Jianhui Lan, Xiaofei Jing, Wenchuan Wang, Jun Xu, Feng Deng, Jason M. Simmons, Shilun Qiu,\* and Guangshan Zhu\*

Porous materials have been of intense scientific and technological interest because of their vital importance in many applications such as catalysis, gas separation, and gas storage.<sup>[1]</sup> Great efforts in the past decade have led to the production of highly porous materials with large surface areas. In particular, the development of metal–organic frameworks (MOFs) has been especially rapid.<sup>[2]</sup> Indeed, the highest surface area reported to date is claimed for a recently reported MOF material UMCM-2, which has a N<sub>2</sub> uptake capacity of 1500 cm<sup>3</sup> g at saturation, from which a Langmuir surface area of 6060 m<sup>2</sup> g (Brunauer–Emmett–Teller (BET) surface area of 5200 m<sup>2</sup> g) can be derived.<sup>[3]</sup> Unfortunately, the high-surface-area porous MOFs usually suffer from low thermal and hydrothermal stabilities, which severely limit their applications, particularly in industry.<sup>[4]</sup> These low stability issues could be resolved by replacing coordination bonds with stronger covalent bonds, as observed in covalent organic frameworks (COFs) or porous organic polymers.<sup>[5]</sup>

However, the COFs and porous organic polymers reported to date have lower surface areas compared to MOFs; the highest reported surface area for a COF is 4210 m<sup>2</sup> g (BET) in COF-103.<sup>[5f]</sup> Thus, further efforts are required to explore various strategies to achieve higher surface areas in COFs. Herein, we present a strategy that has enabled us to achieve, with the aid of computational design, a structure that possesses by far the highest surface area reported to date, as well as exceptional thermal and hydrothermal stabilities. We report the synthesis and properties of a porous aromatic framework PAF-1, which has a Langmuir surface area of 7100 m<sup>2</sup> g. Besides its exceptional surface area, PAF-1 outperforms highly porous MOFs in thermal and hydrothermal stabilities, and demonstrates high uptake capacities for hydrogen (10.7 wt% at 77 K, 48 bar) and carbon dioxide (1300 mg g<sup>-1</sup> at 298 K, 40 bar). Moreover, the super hydrophobicity and high surface area of PAF-1 result in unprecedented uptake capacities of benzene and toluene vapors at room temperature.

It is well known that one of the most stable compounds in nature is diamond, in which each carbon atom is tetrahedrally connected to four neighboring atoms by covalent bonds (Figure 1a). Conceptually, replacement of the C–C covalent bonds of diamond with rigid phenyl rings should not only retain a diamond-like structural stability but also allow sufficient exposure of the faces and edges of phenyl rings with the expectation of increasing the internal surface areas. By employing a multiscale theoretical method,<sup>[6]</sup> which

[\*] T. Ben, H. Ren, X.-F. Jing, Prof. S.-L. Qiu, Prof. G. S. Zhu  
State Key Laboratory of Inorganic Synthesis and  
Preparative Chemistry, Jilin University, Changchun (China)  
Fax: (+86) 431-8516-8331  
E-mail: sqiu@jlu.edu.cn  
zhugs@jlu.edu.cn

S. Ma  
Chemical Sciences and Engineering Division  
Argonne National Laboratory  
9700 S. Cass Avenue, Argonne, IL 60439 (USA)

Prof. D.-P. Cao, J.-H. Lan, Prof. W.-C. Wang  
Key Lab for Nanomaterials  
Beijing University of Chemical Technology, Beijing (China)

J. Xu, Prof. F. Deng  
State Key Lab of Magnetic Resonance and Atomic and Molecular  
Physics  
Wuhan Institute of Physics and Mathematics, Wuhan (China)

Prof. J. M. Simmons  
NIST Center for Neutron Research  
National Institute of Standards and Technology  
Gaithersburg, MD 20899-8562 (USA)

[\*\*] The study was supported by the Outstanding Young Scientist Foundation of the NSFC (20625102), the International Science and Technology Cooperation Program (2007DFA40830), the State Basic Research Project (2006CB806100), NSFC, the “111” Program of Ministry of Education and the Jilin Province Hi-Tech Development Project. S.M. acknowledges the Director’s Postdoctoral Fellowship from the Argonne National Laboratory. J.M.S. acknowledges support from the National Research Council Research Associates Program and the U.S. Department of Energy.

Supporting information for this article is available on the WWW under <http://dx.doi.org/10.1002/anie.200904637>.

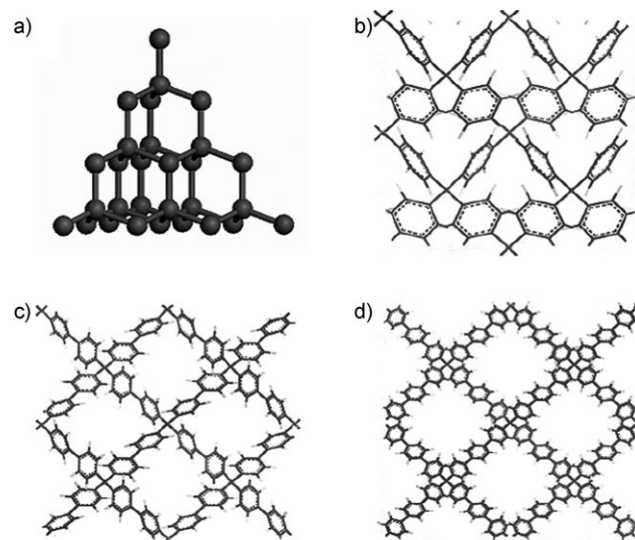
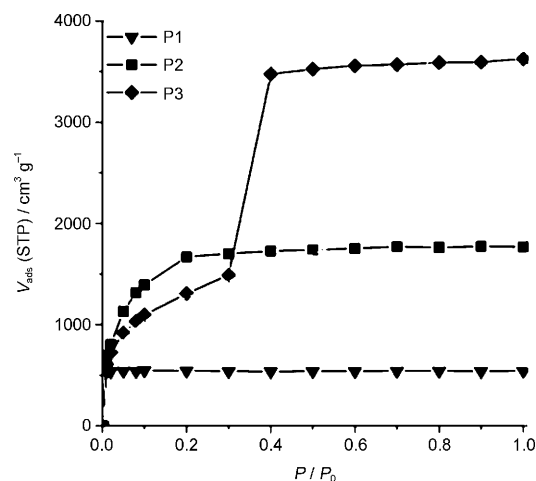


Figure 1. a) structure of diamond; b) structure model of P1; c) structure model of P2; d) structure model of P3.

combines first-principles calculations and grand canonical Monte Carlo simulation (see the Supporting Information), our computational studies indicate that replacement of the C–C bond with one phenyl ring (Figure 1b) can result in a structure (denoted as P1) with a Langmuir surface area of 2350 m<sup>2</sup>g (BET surface area, 1880 m<sup>2</sup>g) and density of 0.8364 g cm<sup>-3</sup>, assuming the preservation of diamondoid topology. Addition of one more phenyl ring to the C–C bond (Figure 1c) can then almost triple the Langmuir surface area to 7000 m<sup>2</sup>g (BET surface area 5640 m<sup>2</sup>g) as well as significantly reducing the density of the structure (denoted as P2) to 0.315 g cm<sup>-3</sup>. Replacement of the C–C bond with three phenyl rings (Figure 1d), however, will enlarge the pore sizes of the structure (denoted as P3) to the mesoscale range, and type IV sorption isotherms can be predicted based on the simulation (Figure 2).

The theoretical simulation results motivated us to seek approaches to synthesize these structures. Since type I sorption isotherms are preferred for small gas molecule storage applications, in particular H<sub>2</sub>, we focus here on the synthesis and properties of the P2 structure. Efforts are also underway for the successful synthesis of the P1 and P3 structures. To synthesize P2, we selected tetrakis(4-bromophenyl)methane<sup>[7]</sup> as the tetrahedral building unit, and the phenyl rings were coupled using the nickel(0)-catalyzed Yamamoto-type<sup>[8]</sup> Ullmann cross-coupling reaction<sup>[9]</sup> (see the Experimental Section). This reaction produced an off-white powdered compound PAF-1, which has a low density and is not soluble in any common organic solvents.

The reaction process can be monitored by FTIR measurements. The spectra clearly indicate the disappearance of the C–Br bonds (Figure S4 in the Supporting Information), thus demonstrating the success of the phenyl–phenyl coupling. To further reveal the local structure of PAF-1, we performed both <sup>1</sup>H and <sup>13</sup>C solid-state NMR studies. As shown in Figure 3a, two major signals at  $\delta = 7.9$  and 7.6 ppm are distinguishable in the <sup>1</sup>H MAS NMR spectrum. These chemical shifts are similar to those of the two types of phenyl protons in the 4,4'-dimethylbiphenyl molecule. The two minor signals at  $\delta = 0.9$  and 1.3 ppm arise from the residual solvent in the sample. The <sup>13</sup>C CP-MAS NMR spectrum of the sample gives more structural information (Figure 3b). The signals at approximately  $\delta = 146$ , 140, 131, 125, and 64 ppm are resolved, and indicate the presence of five different



**Figure 2.** Theoretically calculated N<sub>2</sub> adsorption isotherms at 77 K for P1, P2, and P3. STP=standard temperature and pressure.

carbon atoms in the sample. In addition, the <sup>13</sup>C chemical shifts of the signals are similar to those of the phenyl carbon atoms in the 4,4'-dimethylbiphenyl molecule. Therefore, the two intense signals at  $\delta = 131$  and 125 ppm can be unambiguously assigned to C3 and C4 respectively in the benzene ring, while the two relatively weaker signals at  $\delta = 140$  and 146 ppm are attributed to C2 and C5, respectively (Figure 3c, inset). Since the C3 and C4 atoms are directly connected to protons, the two signals  $\delta = 131$  and 125 ppm exhibit a much stronger cross polarization (CP) enhancement with respect to the two signals at  $\delta = 140$  and 146 ppm. The weak <sup>13</sup>C signal at

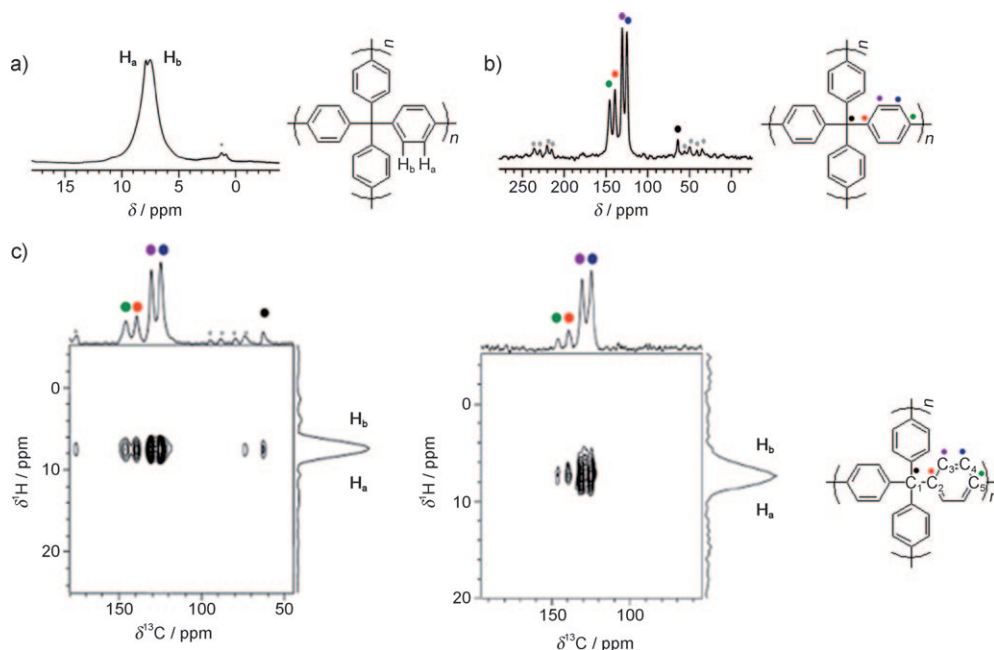


**Figure 3.** a) <sup>1</sup>H MAS NMR spectrum of PAF-1 sample; b) <sup>1</sup>H–<sup>13</sup>C CP/MAS NMR spectrum of the sample with contact time = 4 ms; c) <sup>1</sup>H–<sup>13</sup>C HETCOR spectra of PAF-1 sample recorded with ct = 5 ms, spinning speed of 5 kHz (left) and ct = 0.3 ms, spinning speed of 9 kHz (right). Asterisks denote spinning sidebands. The insets show local structures of PAF-1 as revealed by NMR studies.

approximately  $\delta = 64$  ppm can be assigned to the quaternary carbon atom (C1) that is connected to four phenyl groups. On the basis of the  $^1\text{H}$  and  $^{13}\text{C}$  NMR spectra, the structural unit of the sample can be confirmed. Furthermore, the above assignments are also supported by 2D  $^1\text{H}$ - $^{13}\text{C}$  HETCOR spectra, in which the correlations between the protons and the carbon atoms in spatial proximity are revealed (Figure 3c), that is, the correlation peak between the quaternary carbon and the phenyl proton is only visible with a relatively long contact time (5 ms) because of the large H-C distance.

The above results strongly indicate that the local bonding within PAF-1 agrees well with the structure of P2. In order to probe the long-range structure of PAF-1, powder X-ray diffraction (PXRD) and transmission electron microscopy (TEM) were performed. The PXRD pattern (Figure S7 in the Supporting Information) shows that the main features are consistent with those simulated from the P2 structure, although the peaks are broad, which indicates a highly disordered structure. The high-resolution TEM images (Figure S8 in the Supporting Information) indicate that the texture is largely amorphous but with uniform pore diameter. Although PAF-1 does not possess the long-range crystallographic order present in the proposed P2 structure, we expect the local structure to support a high surface area, as predicted by the theoretical calculations. To investigate its surface area, a fresh PAF-1 sample was fully activated at 200°C under dynamic vacuum for 24 h to remove the guest solvent molecules, and the  $\text{N}_2$  sorption isotherms were measured at 77 K. As shown in Figure 4a, PAF-1 exhibits an exceptionally high  $\text{N}_2$  uptake of  $2000 \text{ cm}^3 \text{ g}^{-1}$  at  $P/P_0 = 0.94$ . When the Langmuir model with a pressure range of  $P/P_0 = 0.05$  to 0.2 is applied, the apparent surface area of PAF-1 is  $7100 \text{ m}^2 \text{ g}^{-1}$  (or using the BET model within the same pressure range, the calculated BET surface area is  $5600 \text{ m}^2 \text{ g}^{-1}$ ). To verify the reproducibility of this  $\text{N}_2$  sorption result, we repeated  $\text{N}_2$  measurements five times using samples prepared from different batches with amounts ranging from 100 mg to 300 mg. The average  $\text{N}_2$  uptake value is  $(2005 \pm 50) \text{ cm}^3 \text{ g}^{-1}$  (error bar in Figure 4a is one standard deviation) at  $P/P_0 = 0.94$ . The apparent surface area of PAF-1 is, to the best of our knowledge, by far the highest among all porous materials reported to date. Remarkably, the apparent surface area of PAF-1 exceeds that of some of the highest surface areas of MOFs, such as MOF-177 ( $4500 \text{ m}^2 \text{ g}^{-1}$ , Langmuir)<sup>[10]</sup> and MIL-101 ( $5900 \text{ m}^2 \text{ g}^{-1}$ , Langmuir),<sup>[11]</sup> as well as a recently reported 3-D COF, COF-103 ( $4210 \text{ m}^2 \text{ g}^{-1}$ , BET).<sup>[5f]</sup> A table comparing similar materials is given in the Supporting Information (Table S3). The surface area of PAF-1 is consistent with the theoretically calculated surface area of the proposed P2 structure (Figure 4), thus providing further evidence of their structural similarity.

Encouraged by the above results, we decided to investigate the structural stability of PAF-1. Thermogravimetric analysis (TGA) indicates that PAF-1 is thermally stable up to 520°C in air (Figure S5 in the Supporting Information). In addition, hydrothermal stability studies on PAF-1 demonstrate that it can retain its structural integrity even after boiling in water for seven days, as indicated by virtually no drop of its  $\text{N}_2$  uptake capacity at 77 K (Figure S6 in the

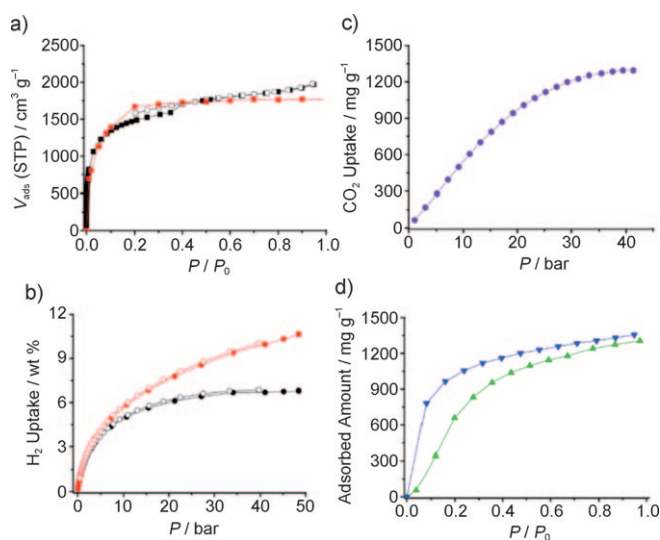


**Figure 4.** a) Experimental adsorption (black square) and desorption (empty square), and simulated  $\text{N}_2$  adsorption (red square) isotherms of PAF-1 at 77 K. b) High-pressure hydrogen sorption isotherms at 77 K. Filled black circle: excess adsorption; empty black circle: excess desorption; filled red circle: total adsorption; empty red circle: total desorption; c) Excess high-pressure carbon dioxide adsorption isotherm at 298 K; d) Benzene (green triangle) and toluene (inverted blue triangle) vapor adsorption isotherms at 298 K.

Supporting Information). These stabilities are superior to high-surface area MOF materials.<sup>[3,10]</sup>

The excellent stability together with its exceptional  $\text{N}_2$  adsorption capacity makes PAF-1 a very attractive candidate for gas storage applications, particularly hydrogen storage and carbon dioxide capture, which are related to clean energy issues. To evaluate the hydrogen storage performance of PAF-1, high-pressure hydrogen sorption isotherms at 77 K were measured using a Sievert apparatus. As shown in Figure 4b, the excess hydrogen uptake capacity of PAF-1 at 48 bar, 77 K can reach 7.0 wt %, which corresponds to an absolute uptake of 10.7 wt %. The  $\text{H}_2$  capacity in PAF-1 is comparable to the best performances of high-surface-area porous MOFs and COFs (Table S3 in the Supporting Information),<sup>[12,13]</sup> and is the highest value among porous organic polymers.<sup>[14]</sup> From the high-pressure hydrogen sorption isotherm data of PAF-1, the isosteric heats of adsorption were calculated using the method described by Zhou et al.<sup>[15]</sup> The zero-loading  $Q_{st}$  was approximately  $4.6 \text{ kJ mol}^{-1}$ , and shows little loading dependence. This observation is consistent with sorption on a homogeneous porous material<sup>[16]</sup> and further supports the role of surface area on the total  $\text{H}_2$  uptake. A high-pressure  $\text{CO}_2$  adsorption isotherm was also collected at 298 K to assess the potential of PAF-1 for carbon dioxide capture applications. As indicated in Figure 4c, PAF-1 can adsorb  $1300 \text{ mg g}^{-1}$   $\text{CO}_2$  at 40 bar and room temperature, which is slightly lower than post-treated MIL-101,<sup>[17]</sup> but is still among the highest for reported porous materials.

Given the aromatic framework of PAF-1, together with its exceptional surface area, we also explored the capability of PAF-1 for adsorption of organic vapors such as benzene and toluene, which are of concern to the environment. As

indicated in Figure 4d, PAF-1 can adsorb large amounts of benzene and toluene vapor at room temperature, with values of  $1306 \text{ mg g}^{-1}$  ( $16.74 \text{ mmol g}^{-1}$ ) and  $1357 \text{ mg g}^{-1}$  ( $14.73 \text{ mmol g}^{-1}$ ), respectively, at saturated vapor pressures. The excellent sorption performances of PAF-1, which widely surpasses those of all other porous materials including hydrogen-bonded cocrystals,<sup>[18]</sup> promises a great potential for the further environmental application of this material.

In conclusion, with the assistance of computational design, a porous aromatic framework with an unprecedented high surface area of  $7100 \text{ m}^2 \text{ g}^{-1}$  has been successfully synthesized. PAF-1 possesses local diamond-like tetrahedral bonding of tetraphenylene methane building units to produce exceptional thermal and hydrothermal stabilities. In addition, PAF-1 demonstrates high uptake capacities of hydrogen and carbon dioxide, as well as benzene and toluene vapors. The strategy presented in this work opens a new avenue for the design and construction of highly porous materials with exceptional stabilities for clean energy and environmental applications.

## Experimental Section

Synthesis of PAF-1: 1,5-cyclooctadiene (cod, 1.05 mL, 8.32 mmol, Aldrich, dried over  $\text{CaH}_2$ ) was added to a solution of bis(1,5-cyclooctadiene)nickel(0) ( $[\text{Ni}(\text{cod})_2]$ , 2.25 g, 8.18 mmol, Aldrich<sup>[19]</sup>) and 2,2'-bipyridyl (1.28 g, 8.18 mmol, Aldrich) in dehydrated DMF (120 mL, Aldrich), and the mixture was heated at  $80^\circ\text{C}$  for 1 h. To the resulting purple solution was added tetrakis(4-bromophenyl)methane (1 g, 1.57 mmol) at  $80^\circ\text{C}$ , and the mixture was stirred at the temperature overnight to obtain a deep purple suspension. After cooling to room temperature, concentrated HCl was added to the mixture. After filtration, the residue was washed with  $\text{CHCl}_3$  ( $5 \times 30 \text{ mL}$ ), THF ( $5 \times 30 \text{ mL}$ ) and  $\text{H}_2\text{O}$  ( $5 \times 30 \text{ mL}$ ), respectively, and dried in vacuo to give PAF-1 as an off-white powder (390 mg, 78% yield). Elemental analysis calcd (%) for  $\text{C}_{25}\text{H}_{16}$ : C 94.94, H 5.06; found: C 94.73, H 5.27; IR (KBr):  $\nu = 3030, 1498, 1004, 812, 705 \text{ cm}^{-1}$ .

NMR experiments: All NMR experiments were performed on a Varian Infinity-plus 400 spectrometer operating at a magnetic field strength of 9.4 T. The resonance frequencies at this field strength were 100.6 and 400.1 MHz for  $^{13}\text{C}$  and  $^1\text{H}$ , respectively. A Chemagnetics 5 mm triple-resonance MAS probe was used to acquire  $^1\text{H}$  and  $^{13}\text{C}$  NMR spectra, with spinning rates of 5–9 kHz.  $^1\text{H}$  MAS NMR experiments were recorded with a windowed phase modulated Lee–Goldburg decoupling sequence (wpmLG) to improve the  $^1\text{H}$  resolution. For the  $^1\text{H}$ – $^{13}\text{C}$  CP/MAS NMR experiments, the Hartmann–Hahn condition was achieved using hexamethylbenzene (HMB), with a contact time (ct) of 4.0 ms and a repetition time of 2.0 s. Two-dimensional  $^1\text{H}$ – $^{13}\text{C}$  CP/MAS heteronuclear correlation (HETCOR) experiments with Lee–Goldburg (LG)  $^1\text{H}$  homonuclear decoupling during the  $t_1$  evolution period were performed using standard methods. Typically 200 scans were acquired for each  $t_1$  increment and the recycle delay was 2 s. The chemical shifts were externally referenced to hexamethylbenzene for  $^{13}\text{C}$  and tetramethylsilane for  $^1\text{H}$ .

Received: August 20, 2009

Published online: November 17, 2009

**Keywords:** adsorption · carbon dioxide · hydrogen · organic frameworks · porous materials

- [1] M. E. Davis, *Nature* **2002**, *417*, 813–821.
- [2] J. R. Long, O. M. Yaghi, *Chem. Soc. Rev.* **2009**, *38*, 1213–1214.
- [3] K. Koh, A. G. Wong-Foy, A. J. Matzger, *J. Am. Chem. Soc.* **2009**, *131*, 4184–4185.
- [4] A. U. Czaja, N. Trukhan, U. Muller, *Chem. Soc. Rev.* **2009**, *38*, 1284–1293.
- [5] a) M. Mastalerz, *Angew. Chem.* **2008**, *120*, 453–455; *Angew. Chem. Int. Ed.* **2008**, *47*, 445–447; b) C. Weder, *Angew. Chem.* **2008**, *120*, 456–458; *Angew. Chem. Int. Ed.* **2008**, *47*, 448–450; c) J.-X. Jiang, F. Su, A. Trewin, C. D. Wood, N. L. Campbell, H. Niu, C. Dickinson, A. Y. Ganin, M. J. Rosseinsky, Y. Z. Khimyak, A. I. Cooper, *Angew. Chem.* **2007**, *119*, 8728–8732; *Angew. Chem. Int. Ed.* **2007**, *46*, 8574–8578; d) E. Stöckel, X. Wu, A. Trewin, C. D. Wood, R. Clowes, N. L. Campbell, J. T. A. Jones, Y. Z. Khimyak, D. J. Adams, A. I. Cooper, *Chem. Commun.* **2009**, 212–214; e) A. P. Côté, A. I. Benin, N. W. Ockwig, M. O’Keeffe, A. J. Matzger, O. M. Yaghi, *Science* **2005**, *310*, 1166–1170; f) H. M. El-Kaderi, J. R. Hunt, J. L. Mendoza-Cortés, A. P. Côté, R. E. Taylor, M. O’Keeffe, O. M. Yaghi, *Science* **2007**, *316*, 268–272.
- [6] D. P. Cao, J. H. Lan, W. C. Wang, B. Smit, *Angew. Chem.* **2009**, *121*, 4824–4827; *Angew. Chem. Int. Ed.* **2009**, *48*, 4730–4733.
- [7] M. Grimm, B. Kirste, H. Kurreck, *Angew. Chem.* **1986**, *98*, 1095–1099; *Angew. Chem. Int. Ed. Engl.* **1986**, *25*, 1097–1098.
- [8] T. Yamamoto, *Bull. Chem. Soc. Jpn.* **1999**, *72*, 621–638.
- [9] G. Zhou, M. Baumgarten, K. Müllen, *J. Am. Chem. Soc.* **2007**, *129*, 12211–12221.
- [10] H. K. Chae, D. Y. Siberio-Perez, J. Kim, Y. Go, M. Eddaoudi, A. J. Matzger, M. O’Keeffe, O. M. Yaghi, *Nature* **2004**, *427*, 523–527.
- [11] G. Ferey, C. Merlot-Draznieks, C. Serre, F. Millange, J. Dutour, S. Surble, I. Margiolaki, *Science* **2005**, *309*, 2040–2042.
- [12] M. Latroche, S. Surble, C. Serre, C. Mellot-Draznieks, P. L. Llewellyn, J. S. Chang, S. H. Jhung, G. Ferey, *Angew. Chem.* **2006**, *118*, 8407–8411; *Angew. Chem. Int. Ed.* **2006**, *45*, 8227–8231.
- [13] L. J. Murray, M. Dinc, J. R. Long, *Chem. Soc. Rev.* **2009**, *38*, 1294–1314.
- [14] A. I. Cooper, *Adv. Mater.* **2009**, *21*, 1291–1295.
- [15] W. Zhou, H. Wu, M. R. Hartman, T. Yildirim, *J. Phys. Chem. C* **2007**, *111*, 16131–16137.
- [16] O. Hübner, A. Glöss, M. Fichtner, W. Klopffer, *J. Phys. Chem. A* **2004**, *108*, 3019–3023.
- [17] P. L. Llewellyn, S. Bourrelly, C. Serre, A. Vimont, M. Daturi, L. Hamon, G. De Weireld, J.-S. Chang, D.-Y. Hong, Y. K. Hwang, S. H. Jhung, G. Frey, *Langmuir* **2008**, *24*, 7245–7250.
- [18] a) V. R. Pedireddi, S. Chatterjee, A. Ranganathan, C. N. R. Rao, *J. Am. Chem. Soc.* **1997**, *119*, 10867–10868; b) A. Ranganathan, V. R. Pedireddi, S. Chatterjee, C. N. R. Rao, *J. Mater. Chem.* **1999**, *9*, 2407–2411.
- [19] Certain commercial suppliers are identified in this paper for information purposes. Such identification does not imply recommendation or endorsement by the National Institute of Standards and Technology, nor does it imply that the materials or equipment identified are necessarily the best available for the purpose.